

# A case study on different one-factor Cheyette models for short maturity caplet calibration

Arun Kumar Polala, Bernhard Hientzsch

August 22, 2024

## Abstract

In [PH23], we calibrated a one-factor Cheyette SLV model with a local volatility that is linear in the benchmark forward rate and an uncorrelated CIR stochastic variance to 3M caplets of various maturities. While caplet smiles for many maturities could be reasonably well calibrated across the range of strikes, for instance the 1Y maturity could not be calibrated well across that entire range of strikes. Here, we study whether models with alternative local volatility terms and/or alternative stochastic volatility or variance models can calibrate the 1Y caplet smile better across the strike range better than the model studied in [PH23]. This is made possible and feasible by the generic simulation, pricing, and calibration frameworks introduced in [PH23] and some new frameworks presented in this paper. We find that some model settings calibrate well to the 1Y smile across the strike range under study. In particular, a model setting with a local volatility that is piece-wise linear in the benchmark forward rate together with an uncorrelated CIR stochastic variance and one with a local volatility that is linear in the benchmark rate together with a correlated lognormal stochastic volatility with quadratic drift (QDLNSV) as in [SR23a] calibrate well. We discuss why the later might be a preferable model.

## 1 Introduction

In [PH23], we proposed and tested a new calibration methodology on the example of 3M caplets of various maturities, calibrating one-factor Cheyette models with a local volatility that is linear in the 3M forward rate and an uncorrelated CIR stochastic variance. While most maturities could be calibrated reasonably well across a range of strikes, the 1Y maturity could not be calibrated well across the entire range of those strikes. When calibrating the wings reasonably well, strikes in the range of about 200bps to 300bps – right of ATM – could not be calibrated well, see Figure 1.

Here, we study whether one-factor Cheyette models with different forms of local volatilities and/or stochastic volatilities or variances will calibrate better. We find that some model settings calibrate well, in particular, a model setting with a local volatility that is piece-wise linear in the benchmark forward rate together with an uncorrelated CIR stochastic variance and one with a local volatility that is linear in the benchmark rate together with a correlated lognormal stochastic volatility with quadratic drift (QDLNSV) as in [SR23a] lead to good calibrations. We see that the presented generic simulation, pricing, and calibration frameworks make such calibration and modeling studies, feasible, efficient, and even easy and can serve as a good foundation for modeling.

The paper is organized as follows: In section 2, we introduce the Cheyette models under consideration, including motivation for and references for the various forms. In section 3, we

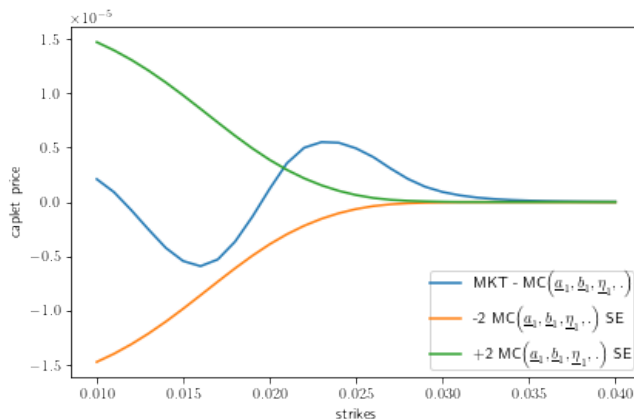


Figure 1: Calibrating the 1yr Maturity Caplet smile, Cheyette Model with Linear Benchmark Forward Rate Local Volatility and CIR SV. Figure and data from [PH23]. Shown is difference between model price (MC) and market price (MKT), MC error bars are shown for comparison.

introduce caplets and floorlets and how they can be priced in the Cheyette model by simulation. We then introduce the Generic Simulation Framework in section 4 which allows us to simulate various payoffs under various models, including under varying parameters, in a convenient and efficient fashion. In section 5, we present how the Generic Simulation Framework can be used to code generate MC pricers for various backends (TensorFlow, NumPy, JAX) and how calibration can be implemented by optimization around such pricers. In section 6, we discuss how the recently proposed parametric differential machine learning (PDML) methodology can be used for such parametric pricing and calibration. In section 7, we quickly discuss when to apply code generation versus PDML approaches for the parametric pricers. Finally, in section 8, we apply these pricing and calibration methods to calibrate Cheyette models in various model settings, inspect the results, and identify the best models for our purposes. In section 9, we conclude.

## 2 One factor Cheyette Models

The dynamics of a single factor Cheyette model with states  $\{x_t, y_t\}$ , volatility process  $\sigma_t$ , and constant mean reversion is given by

$$dx_t = \mu_t dt + \sigma_t dW_t, \quad (1)$$

$$dy_t = (\sigma_t^2 - 2\lambda y_t) dt, \quad (2)$$

where  $\lambda$  is mean reversion speed and  $W_t$  is a standard Brownian motion.  $x_t$  is the diffusive Cheyette factor while  $y_t$  is a locally deterministic auxiliary factor ensuring that the curve stays arbitrage free. The drift term  $\mu_t$  is given by

$$\begin{aligned} \mu_t &= (y_t - \lambda x_t) \quad (\text{risk neutral measure}), \\ &= (y_t - \lambda x_t - G(T-t)\sigma_t^2) \quad (\text{T-Fwd measure}), \end{aligned} \quad (3)$$

where  $G(x) = \frac{1-h(x)}{\lambda}$  and  $h(x) = e^{-\lambda x}$ . In this paper, we use  $\lambda = 0.03$ , a common value from the literature. The choice of  $\lambda$  does not seem to impact the results too much beyond numerical

stability. Thus, we are using a standard, stable value. The volatility process  $\sigma_t$  is specified as follows:

$$\begin{aligned}\sigma_t &= \sigma(t, x_t, y_t) \quad (\text{no SV}), \\ &= \sigma(t, x_t, y_t)\vartheta_t \quad (\text{SV}),\end{aligned}\tag{4}$$

where  $\vartheta_t$  is some stochastic process. In this paper, we consider the following functional forms for the local volatility function  $\sigma(t, x_t, y_t)$ :

(i) Linear short rate volatility ('LinSRLV'):

$$\sigma(t, x_t, y_t) = a + b \times (f(0, t) + x_t),\tag{5}$$

where  $f(0, t)$  is the initial forward rate. This form has been used, for instance, by [Hoo11], both without stochastic volatility or variance and with uncorrelated CIR stochastic variance. Short(est) maturity rates can be observed in the market or extracted from discount curves which are constructed and saved at least every business day in financial institutions and can be analyzed over time. It is typically assumed that the historical evolution of risk factors and the risk neutral evolution as implied from traded options are equivalent with a measure change involving various market prices of risk which change the drift but not the volatility during the measure change. Hence, observed behaviors of the volatility of the short rate or of another rate can inform the structure of the volatility term. The volatility of the observed short rate seems to be linear in the short rate within certain regimes.

(ii) Linear benchmark forward rate volatility ('LinBRLV'):

$$\sigma(t, x_t, y_t) = a + b \times f(t, t + \delta),\tag{6}$$

where  $f(t, t + \delta)$  is the forward rate for tenor  $\delta$  and can be computed as follows:

$$f(t, t + \delta) = f(0, t + \delta) + h(\delta)(x_t + y_t G(\delta)).\tag{7}$$

This form is the "standard form" advocated for and used by [AP10] and many in industry and academia, both without stochastic volatility or variance and with uncorrelated CIR stochastic variance.

(iii) Volatility linear in Cheyette factor ('LinXLV'):

$$\sigma(t, x_t, y_t) = a + b \times x_t.\tag{8}$$

This form has been used and advocated for in [Chi12].

(iv) Piece-wise linear benchmark forward rate volatility ('PwLinBRLV'):

$$\begin{aligned}\sigma(t, x_t, y_t) &= a_1 1_{f(t, t + \delta) < K_1} + \sum_{i=1}^{n-1} (a_i + b_i (f(t, t + \delta) - K_i)) 1_{K_i \leq f(t, t + \delta) < K_{i+1}} \\ &\quad + a_n 1_{K_n \leq f(t, t + \delta)},\end{aligned}\tag{9}$$

where  $\{K_i\}_{i=1}^{i=n}$  denotes the set of strikes in increasing order,  $b_i = \frac{a_{i+1} - a_i}{K_{i+1} - K_i}$ , and  $\{a_i\}_{i=1}^{i=n}$  denotes the constant terms.

As discussed above, studying how the volatility of the rates behaves under the historical measure can inform the volatility models under pricing measure since the processes under

two equivalent measures would share the same volatility term (but not drift). [DRP13] studied the volatility of interest rates in particular in dependence of the rate level and found a piece-wise-linear form to be a good approximation over a very long observation period in various rate regimes. Thus, local volatilities for benchmark instantaneous forward rates, piece-wise linear in said benchmark forward rates; or local volatilities for short rates, piece-wise linear in short rates, would be supported by the studies in [DRP13].

For the stochastic volatility or variance (SV) dynamics, we consider two types of stochastic models: CIR stochastic variance and lognormal stochastic volatility with quadratic drift ('QDLNSV'). These two models and other SV models were compared in [SR23b]. In this paper, we investigate CIR SV and lognormal SV with quadratic drift (QDLNSV) in the context of the Cheyette model. The stochastic processes  $\vartheta_t$  for CIR SVs and lognormal SV with quadratic drift is given below:

- CIR stochastic variance ('CIRSV'): Here,  $\vartheta_t = \sqrt{z_t}$  with an SDE for  $z_t$ :

$$dz_t = \theta(z_0 - z_t)dt + \eta(t)\sqrt{z_t}dZ_t, \quad (10)$$

where  $\theta$  is the mean reversion speed of variance,  $\eta(t)$  is volatility of variance,  $z_0 = z(0) = 1$ , and we assume  $dZ_t dW_t \equiv 0$ . We are using  $\theta = 0.2$ , but we confirmed that the calibration results are not sensitive to the exact value of the mean reversion speed of the variance. For CIR SV models, we have the Feller condition which says that only if twice the product of mean reversion speed ( $\theta$ ) and long-term mean (here,  $z_0 = 1$ ) is larger than the square of the volatility coefficient  $\eta(t)$  is the process  $z_t$  positive ( $2\theta z_\infty \geq \eta^2$  with  $z_\infty = z_0$  here). If the Feller condition is not satisfied,  $z_t$  can be zero, can spend substantial time absorbed in or close to zero, and will behave deterministically in the first instant after hitting zero, contradicting for many what seems to be observed in the market. If either the local or the stochastic volatility term is zero, the volatility term will be zero, and thus Girsanov transformations cannot change the drift, leading to additional modeling restrictions when modeling behavior both in the observational measure and pricing measure with a standard risk neutral pricing approach. In this paper, we enforce the Feller condition in the calibrations.

- Correlated CIR SV ('CorCIRSV'): Here, still  $\vartheta_t = \sqrt{z_t}$  with an SDE for  $z_t$ , but nonzero correlation is allowed. Under risk-neutral measure, the SDE is given as:

$$dz_t = [\theta(z_0 - z_t)]dt + \beta(t)\sqrt{z_t}dW_t + \epsilon(t)\sqrt{z_t}dW_t, \quad (11)$$

while under  $T$ -forward measure it is given as:

$$dz_t = [\theta(z_0 - z_t) - G(T-t)\sigma(t, x_t, y_t)\beta(t)z_t]dt + \beta(t)\sqrt{z_t}dW_t + \epsilon(t)\sqrt{z_t}dW_t, \quad (12)$$

where  $\theta$  is the mean reversion speed of variance,  $\eta(t)$  is volatility of variance,  $\beta(t) = \rho\eta(t)$ ,  $\epsilon(t) = \sqrt{1 - \rho^2}\eta(t)$ , and  $z_0 = z(0) = 1$ , and we assume  $dZ_t dW_t \equiv \rho$ . We are using  $\theta = 0.2$  as in the uncorrelated case above and the same Feller condition applies (and is enforced in the calibrations). As can be seen, non-zero correlation leads to additional drift terms under  $T$ -forward and annuity measures which means that the standard approximations leading to displaced Heston models do not apply, and the approximate fast solvers proposed for the zero correlation case cannot be applied.

- Lognormal stochastic volatility with quadratic drift ('QDLNSV'): Here, an SDE for  $\vartheta_t$  is directly specified. This SDE under the two measures is given as:

$$\begin{aligned}
d\vartheta_t &= (\kappa_1 + \kappa_2\vartheta_t)(\theta - \vartheta_t)dt + \beta(t)\vartheta_t dW_t + \epsilon(t)\vartheta_t dZ_t \quad (\text{under risk neutral}) \\
d\vartheta_t &= ((\kappa_1 + \kappa_2\vartheta_t) \times (\theta - \vartheta_t) - G(T-t)\sigma(t, x_t, y_t)\beta(t)\vartheta_t^2)dt \\
&\quad + \beta(t)\vartheta_t dW_t + \epsilon(t)\vartheta_t dZ_t \quad (\text{under T-Fwd measure}),
\end{aligned}$$

where  $\kappa_1$  and  $\kappa_2$  are linear and quadratic mean reversion speeds, respectively,  $\theta$  is the mean level of volatility,  $\beta(t)$  and  $\epsilon(t)$  are deterministic terms, and we assume  $dZ_t dW_t \equiv 0$ . We follow [SR23a] in that we are choosing to assume  $\kappa_1 = \kappa_2 = \kappa$  to avoid over-parameterization and pick a  $\kappa$  that seems to lead to a calibrated volatility of volatility that is relatively stable across expiries, which seems to be around  $\kappa = 0.25$  for the USD market. We also follow [SR23a] by picking  $\lambda = 0.025$ . As is common in rates and some applications in equity, we use the stochastic volatility only to shape the distribution but not to impact the expected volatility by choosing  $\theta = 1$  and  $\vartheta_0 = 1$ . Note that, in this case we have different dynamics for the stochastic volatility based on the choice of measure just as for correlated CIR SV, whereas in the case of uncorrelated CIR SV the dynamics remains the same irrespective of the measure.

Besides previous work and studies on the volatility of rates in the observational measure, there is another important consideration in the literature when choosing a particular form of local and stochastic volatility or variance. Most papers argue that closed-form or almost closed-form pricers for calibration instruments are required to obtain a calibration that will be fast enough and thus forms are preferred that lead to settings in which such pricers can be found or that can be approximated by settings in which such pricers can be or have been found. (Forward term rate) Caplets and floorlets can often be priced as options on zero-coupon bonds assuming that the underlying model has closed-form or quasi-closed-form solutions for such options. However, caplets and floorlets can also be seen as options on forward rates. The forward term rate under the forward measure corresponding to the payment time (which is equals to the end time of the forward rate) of the caplet is a martingale and the SDE for it can be derived and turns out to be structurally similar to or the same as the SDE for the Cheyette factors. The swap rate under the annuity measure corresponding to the fixed leg of the swap is a martingale and the SDE for it can be derived and turns out to be structurally similar to the SDE for the Cheyette factor. In the swaption case, a number of approximations and assumptions are necessary to approximate the swap rate SDE with an SDE of the same form with constant coefficients. Settings with constant, linear, and quadratic local volatility without stochastic volatility can be solved in (quasi-)closed-form; thus leading to people choosing such local volatility forms and using those solvers. The coefficients of the local volatility form for the swap rate might be time dependent and mildly stochastic but can be approximately reduced by time-averaging to settings with constant coefficients. Settings with constant or linear local volatility with uncorrelated CIR stochastic variance can be mapped to (displaced) Heston and Heston solvers (with direct integration or by FFT or other transform methods) can be used for pricing. While these (displaced) Heston solvers can treat correlation between the underlying and the stochastic variance, assuming such nonzero correlation between the stochastic variance and the Cheyette factor does not allow the approximations and transformations that map the forward rate or swap rate SDE to a displaced Heston model. Theoretically, other uncorrelated stochastic volatility or variance models could be used in a similar fashion assuming that solvers are available and the appropriate forms of time-averaging have been derived, but it seems that no such time-averaging has been published, and such solvers have not been used so far.

Alternatively, one can try to derive approximate solvers by various expansions, for instance as in [SR23a]. This leads to similar needs to derive approximations and expansions and to implement them; while possibly allowing settings in which the stochastic volatility can be correlated to the underlying factor and/or rate.

We here price and calibrate based on MC simulation pricing and are thus not constrained by such considerations as long as the proposed pricing and calibration approaches are fast enough to be used. Since we are pricing under the original, not approximated, problem, we can price arbitrarily well by using enough MC samples assuming the discretization is convergent. Thus, MC simulation is typically used to benchmark approximation approaches as in [SR23a]. We can control accuracy for the calibration pricers by choosing appropriate numbers of samples and other discretization parameters.

### 3 Calibration Instruments: Caplets and Floorlets

(Forward term rate) Caplets and floorlets are European style interest rate derivatives. Let  $T_1 < T_2$ , then the payoff of the caplet and floorlet at  $T_2$  for notional amount  $N$  is

$$N\delta^\omega(T_1, T_2) (\omega (F_{T_1}^F(T_1, T_2) - K))^+, \quad (13)$$

where

$$\begin{aligned} \omega &= 1 \quad (\text{caplet}) \\ &= -1 \quad (\text{floorlet}), \end{aligned} \quad (14)$$

$K$  is the strike price,  $F^F(T_1, T_2)$  is the forward rate for the time period  $[T_1, T_2]$ ,  $T_1$  is the reset date,  $T_2$  is the payment date and  $\delta^\omega$  is an appropriate day count fraction between  $T_1$  and  $T_2$  for the caplet and floorlet.

The forward rate can be computed from the discount factor for the forward/forecasting curve  $P^F(t, T)$  - which represents the discount factor for that curve for  $T$  as seen from  $t$ .

$$F_t^F(t^S, t^E) = \frac{1}{\delta^F(t^S, t^E)} \left( \frac{P^F(t, t^S)}{P^F(t, t^E)} - 1 \right), \quad (15)$$

with  $\delta^F$  being the appropriate day count fraction for the forecasting forward rate.

We consider the two-curve setting, in which the forecasting curve  $P^F$  and the discounting curve  $P^D$  can be different. Based on hypothesis **(S0)** as formalized and introduced in [Hen10], we can write the forward rate based on the forecasting curve as an affine function of the forward rate based on the discounting curve.

$$F_t^F(t^S, t^E) = mF_t^D(t^S, t^E) + s, \quad (16)$$

with

$$m = \beta_0^F(t^S, t^E), \quad (17)$$

$$s = \frac{\beta_0^F(t^S, t^E) - 1}{\delta(t^S, t^E)}, \quad (18)$$

$$\beta_0^F(t^S, t^E) = \frac{P^F(0, t^S) P^D(0, t^E)}{P^F(0, t^E) P^D(0, t^S)}. \quad (19)$$

Here, we assume that the time conventions and day counts for the different curves are the same, i.e.,  $\delta^D = \delta^F = \delta$ . Otherwise, the structure of the formulas stays the same while the exact form of the coefficients becomes somewhat more complicated. For further discussion of this setting and the above expressions, see [PH23].

For the Cheyette models under consideration, the discount factor functions  $P^\cdot(t, T)$  for the two curves (forecasting and discounting) are given as a function of state variables  $(x_t, y_t)$ .

$$P^\cdot(t, T; x_t, y_t) = \frac{P^\cdot(0, T)}{P^\cdot(0, t)} \exp\left(-G(T-t)x_t - \frac{1}{2}G^2(T-t)y_t\right). \quad (20)$$

Note that the discount factor function  $P^\cdot$  depends only on  $(x_t, y_t)$  even in the case of SV. Also, note that  $P^\cdot(0, T; x_0, y_0)$  is equal to the initial curve  $P^\cdot(0, T)$ . Further, the discount factor function remains the same for both measures (T-Fwd and risk neutral), just that  $x_t$  and  $y_t$  are given by SDE systems with different drifts for the different measures.

The payoff of a caplet ( $\omega = 1$ ) and floorlet ( $\omega = -1$ ) given in Equation 13 can be simplified to:

$$N\delta\left(\omega\left(F_{T_1}^F(T_1, T_2) - K\right)\right)^+ = N\left(\omega\left(\frac{m}{P^D(T_1, T_2)} - \hat{K}\right)\right)^+, \quad (21)$$

with

$$\hat{K} = 1 + K\delta. \quad (22)$$

Here, we assume that the day count for the caplet or floorlet ( $\delta^\omega$ ) is the same as the forecasting and discounting forward rate day count ( $\delta$ ). Using the discount factor function given in Equation 20, we can simplify

$$\left(\frac{m}{P^D(T_1, T_2)} - \hat{K}\right) = \left(\frac{P^F(0, T_1)}{P^F(0, T_2)} \exp\left(G(T_2 - T_1)x_{T_1} + \frac{1}{2}G^2(T_2 - T_1)y_{T_1}\right) - \hat{K}\right) \quad (23)$$

and write Equation 21 as:

$$N\left(\omega\left(\frac{m}{P^D(T_1, T_2)} - \hat{K}\right)\right)^+ = N\left(\omega\left(p_F \exp(c_x x_{T_1} + c_y y_{T_1}) - \hat{K}\right)\right)^+, \quad (24)$$

for appropriate coefficients  $p_F$ ,  $c_x$ , and  $c_y$ . For further details, we refer to [PH23].

Finally, the price of a caplet and floorlet as of time 0 is given by

$$\text{Num}_0 \times E\left[\frac{N\left(\omega\left(p_F \exp(c_x x_{T_1} + c_y y_{T_1}) - \hat{K}\right)\right)^+}{\text{Num}_{T_2}}\right], \quad (25)$$

with  $\text{Num}_t$  given by

$$\begin{aligned} \text{Num}_t &= P^D(t, T) \quad \text{under T-Fwd measure,} \\ &= e^{\int_0^t r(u)du} \quad \text{under risk neutral measure.} \end{aligned} \quad (26)$$

In case of forward measure, we chose  $T_2$ -Fwd measure in which case  $\text{Num}_t = P^D(t, T_2)$ . As,  $P^D(T_2, T_2) \equiv 1$  we have  $\text{Num}_{T_2} \equiv 1$  and  $\text{Num}_0 = P^D(0, T_2)$ .

In One-Factor Cheyette models, we can write the short rate  $r$  as follows:

$$r(t) = f(0, t) + x_t. \quad (27)$$

So, under the risk neutral measure the numéraire  $\text{Num}_t$  can be expressed as follows:

$$\text{Num}_t = e^{\int_0^t (f(0,u) + x_u) du}, \quad (28)$$

$$d\text{Num}_t = (f(0,t) + x_t) \text{Num}_t dt. \quad (29)$$

Note that in this case,  $\text{Num}_0 = 1$ . Based on Equation 29, we can jointly simulate  $\text{Num}_t$  along with the state variables  $(x_t, y_t)$  (and volatility variable  $\vartheta_t$  if any). If we include  $T_2$  in the simulation times, we can get  $\text{Num}_{T_2}$  for the simulated sample paths.

## 4 Generic Simulation Scripting Framework

In [PH23], we introduced a generic simulation scripting framework (GenSimFW) to simulate stochastic processes and compute functionals based on observed values of those simulated stochastic processes, starting from a textual description in close-to-mathematical formulation. This script framework can use several backends, currently TensorFlow in computational graph mode, JAX, and NumPy. TensorFlow computational graphs generated by the TensorFlow backend are amenable to TensorFlow computational graph operations such as `tf.gradients` which allow one to augment the computational graph to one that also computes derivatives of specified output values (such as the payoff) with respect to any other node of the computational graph including parameters or inputs. [PH23] used the scripting framework to introduce a new methodology for parametric pricing called parametric differential machine learning which learns conditional expectations given samples of the output random variate and the conditioning variables and the path-wise derivative of the output random variate with respect to the conditioning variables.

We will explain the features of the input script needed to perform the modeling and calibration tests in this paper by discussing the example scripts in Figures 2 and 3. In Figure 2, on the top, there are function definitions for the rest of the script. (The script framework predefines a set of functions that is common to the different backends - such as `exp`, `oneslike`, `zeroslike`, `sqrt`, and `positivepart` as used in the script, but also others such as `einsum`. Other functions that are or can be implemented in the backends together with appropriate derivatives can be added to the framework easily.)

Next, we describe what is simulated and computed at each time-step. If the line starts with `d_`, it describes an increment. In the right-hand side, `d_t` can be used (and will be defined to be the current time step size) and any other name starting with `d_` on the right-hand side stands for a Brownian increment (normal random variate with zero mean and standard deviation of one, potentially correlated with other normal random variates as specified elsewhere in the script) which will be generated and values provided when the right-hand side will be evaluated. Thus, for a description `d_x = rhs`, `x` after the step will be `x+rhs` with `x` the value before the time step. Here, this is how `ratex`, `ratey`, and `ratevariance` will be time-stepped. The other expressions for `ratevolatility`, `deltafwd`, and `volterm` compute these variables as functions of (current values<sup>1</sup> of) other variables, as long as the variable defined in the expression does not also occur on the right hand side expression. Should the variable occur on both sides, it describes a Markovian update function - but they have not been used in the example scripts. An example description that could be added to the example script would be `deltafwdmax=max(deltafwdmax,deltafwd_new)` which would keep the running maximum of `deltafwd` in `deltafwdmax`. Here, if there is a variable name ending in `_new` on the right-hand side, it will receive the new value of that variable, while without `_new` it refers to the old value.

<sup>1</sup>I.e., if values at the end of the time step have already been computed by preceding lines, the value at the end of the time steps is used, otherwise, the value at the beginning of the time step as computed in the previous time step (or as given by or computed from initial values) is used.



Then, the example script in Figure 2 specifies initial values for the time-stepped variables, as indicated by the line starting with `init:`. If initial value for a variable has not been specified, it is computed from the simulation description, if possible; otherwise an error will result.

Finally, a set of payoffs is defined. In the loop form shown in Figure 2, at least one of the loop variables must be `t`, and specifies the payment time for the payoff. The expressions for the values of the loop variable are evaluated when parsing the script (as is the string expression for the name of the payoff), not when the computation described by the parsed script is executed when generating the computational graph or when evaluating the expressions or the computational graph. `nodiscount` means that there is no extra discounting. Instead, one could specify `discount discountfactorexpression` where the payoff would be multiplied with the value of the `discountfactorexpression`. For instance, one could simulate the stochastic discount factor by `d_SDF=-(initfwd(t)+ratex)*SDF*d_t` and use `discount SDF` with `SDF` being the discount factor expression. Alternatively, one could specify `numeraire numeraireexpression`, in which case the payoff would be divided by the value of the `numeraireexpression`. As an example, one could simulate the money market account by `d_MMA = (initfwd(t)+ratex)*MMA*d_t`, and then specify `numeraire MMA`. Instead of using the loop form, one can specify a single payoff as in the examples in [PH23] like:

```
# payoff
maturity: caplet pays positivepart(pf*exp(cx*ratex[fixingtime]+\
                                     cy*ratey[fixingtime])-khat) \
          nodiscount
```

where a definition for `maturity` and `fixingtime` needs to be provided to the scripting framework, and `maturity` (or whatever variable or number given before the `:`) will be used as payment time. In the payoff, square brackets indicate the time at which variables will be observed and then used in the computation.

The next script, Figure 3, also demonstrates the specification of correlations in the line `d_W*d_Z = rho`. The expression on the right-hand side can contain functions, processes, etc. and in this way can use for settings with local or stochastic or mixed local and stochastic correlation.

The script framework also accepts simulations that involve vectors or tensors in the SDEs and also as Brownian increments. For that case, dimensions need to be specified, and there are backend functions (such as `einsum`) that can operate on such vectors or tensors.

The scripting framework also allows the definition of time structured computations where updating of specific variables only occurs at certain time points and not at every time step. As a possible example, one could keep track of a maximum or minimum or sum over values observed at a finite set of given times, or performance for Cliquet like instruments.

For a more formal introduction into the Generic Scripting framework, see [PH23].

In [PH23], we presented a script for caplet pricing for Cheyette model with linear benchmark forward rate local volatility (LinBRLV) with uncorrelated CIR SV. Compared to the script in [PH23], we need to make only minor changes to use other functional forms for the local volatility term or alternative forms of SV. Examples can be found in the scripts that we just discussed to introduce the scripting framework. Figure 2 shows caplet pricing for a Cheyette model with piece-wise linear benchmark forward rate local volatility (PwLinBRLV) together with uncorrelated CIR SV. Figure 3 shows caplet pricing for a Cheyette model with local volatility linear in Cheyette factor  $x$  (LinXLV) together with correlated lognormal SV with quadratic drift (QDLNSV). Note that, in Figures 2 and 3, we price caplets with different strikes simultaneously whereas the scripts in [PH23] show caplet pricing for one strike at a time.

Given the appropriate scripts and set-up information, GenSimFW provides a variety of features for a variety of backends. All start with parsing and preprocessing of the script and

```

# function definition
g(x) = (1/mr)*(oneslike(x)-exp(-mr*x))
h(x) = exp(-mr*x)
sigmaFun1(x) = a1*oneslike(x) if x < K1*oneslike(x) else zeroslike(x)
sigmaFun2(x) = a1 + ((a2 - a1)/(K2 - K1))*(x - K1*oneslike(x)) \
  if x >= K1*oneslike(x) and x < K2*oneslike(x) else zeroslike(x)
sigmaFun3(x) = a2 + ((a3 - a2)/(K3 - K2))*(x - K2*oneslike(x)) \
  if x >= K2*oneslike(x) and x < K3*oneslike(x) else zeroslike(x)
sigmaFun4(x) = a3*oneslike(x) if x >= K3*oneslike(x) else zeroslike(x)

#system
d_ratex = (ratey-mr*ratex-g(measT-t)*ratevariance*volterm*volterm)*d_t+\
  ratevolatility*volterm*d_W
d_ratey = (ratevariance*volterm*volterm-2.0*mr*ratey)*d_t
d_ratevariance = theta*(oneslike(ratevariance) - positivepart(ratevariance))*d_t
  + volofvar*ratevolatility*d_Z
ratevolatility = sqrt(positivepart(ratevariance))
deltafwd = initfwd(t + delta) + h(delta)*(ratex + g(delta)*ratey)
volterm = sigmaFun1(deltafwd) + sigmaFun2(deltafwd) + sigmaFun3(deltafwd) +
  sigmaFun4(deltafwd)

#initial values
init: ratex = zeros([batchsize])
init: ratey = zeros([batchsize])
init: ratevariance = ones([batchsize])

#payoffs
for (t,k) in ([maturity]*len(strikes),strikes): "calloption_strike_\\%f"\\%k \
  pays (positivepart(poa*exp(g(delta)*ratex[t] + \
    0.5*g(delta)*g(delta)*ratey[t]) - 1 - k*delta)) nodiscount

```

Figure 2: Script for Caplet Pricing for Cheyette Model with uncorrelated CIR SV (Euler for Cheyette, Euler full truncation for CIR), with piece-wise linear benchmark forward rate local volatility (PwLinBRLV).

preparing for interpretation or code generation. There is a direct execution mode, in which the parsed script is used to execute TensorFlow computational graph building mode functions to create a computational graph that can be further worked with (such as adding computation of appropriate derivatives) and then run - as in TensorFlow version 1 or the version 1 compatibility layer of TensorFlow version 2, or is used to execute appropriate NumPy or JAX functions. There is also a code generation mode, in which the parsed script is used to generate a Python module containing TensorFlow, NumPy, or JAX calls; which then would create a computational graph (for the TensorFlow backend) or execute the computation (for NumPy and JAX). The basic computation supported currently is simulation and sample generation in batches (including samples of path-wise derivatives generated through augmented computational graphs in TensorFlow or appropriately code generated) either with fixed parameters or with varying parameters for different trajectories in the batch. These samples can either be directly used for training in DML or PDML type approaches or can be used to compute MC estimates for (conditional) expectations and potentially their sensitivities directly by MC averaging. These simulations and MC estimates can also use antithetic variates, control variate approaches, and similar methodologies. There are extensions for calibration, XVA, and Bermudan option exercise strategies and option pricing which we will describe elsewhere.

```

#function def
g(x) = (1/mr)*(oneslike(x)-exp (-mr*x))

#system
d_ratex = (ratey - mr*ratex - g(measT-t)*volterm*volterm*sigma*sigma)*d_t +
    volterm*sigma*d_W
d_ratey = (volterm*volterm*sigma*sigma - 2.0*mr*ratey)*d_t
d_sigma = ((kappa1 + kappa2*sigma)*(1.0 - sigma) - g(measT-t)*volterm*beta*sigma*
    sigma)*d_t + beta*sigma*d_W + eps*sigma*d_Z
volterm = a + b*ratex

#correlations-
d_W*d_Z = rho

#initial values
init: ratex = zeros([batchsize])
init: ratey = zeros([batchsize])
init: sigma = ones([batchsize])

#payoffs
for (t,k) in ([maturity]*len(strikes),strikes): "calloption_strike_\\%f"\\%k \
    pays (positivepart(poa*exp(g(delta)*ratex[t] + \
        0.5*g(delta)*g(delta)*ratey[t] - 1 - k*delta)) nodiscount

```

Figure 3: Script for Caplet Pricing for Cheyette Model with Lognormal SV with quadratic drift (Euler for both Cheyette and QDLNSV) with local volatility linear in the Cheyette factor  $x$  (LinXLV).

## 5 Code generated Monte-Carlo pricers and their use within Calibration

Using GenSimFW as just described, one can execute (or code generate and execute) standard Monte-Carlo pricers that generate MC estimates of prices given parameter values. One could now run global or local optimizers that do not need derivatives (such as variants of differential evolution, for instance, ICDE, but there are other global optimization packages available in open source, for instance DFOLS by NAG) to find optimized parameter sets through minimization of appropriate objective functions.

However, MC estimates are currently rarely used for calibration out of a number of concerns, some related to the inherent complexity while others are related directly to the use of Monte Carlo approaches. For one, calibration can be provided by some monolithic function or program, or it could be provided by some set of components that are appropriately connected and steered. There is also a question about how configurable the monolithic function or components are. Monolithic designs will force more one-off work and even if configurable, all things need to be configured in a monolithic manner. Component-based designs might have to be one-off or partially configurable, but the component design allows one to combine these components more freely. Given the complexity (global/local optimizer, objective function, simulation, post-processing), monolithic designs and components will be very complex yet need to fit together so that work cannot be easily distributed among a team. Monolithic designs also typically generate their random numbers internally and make it harder to split generation and consumption of random numbers, while in a component design, random number generation can be its own component. Therefore, one also encounters a more flexible, component based design, where

components are either one-off or configurable. There has to be a (configurable) layer where these components are combined appropriately for the pricing and calibration tasks at hand. That control component could be a scripting layer embedded in one of the implementation languages (C, C++, etc.) using some scripting functionality; or it could be a Python interface (or another appropriate scripting language) to the components including control component(s). Such a design often also becomes complex and is hard to design, develop, and support; even though typically less complex as in a monolithic design.

Developing, managing, supporting, and using one-off implementations for different models, instruments, and computational architectures (CPUs, GPUs, distributed computing, etc.) will result in a complex setup. It will be difficult and challenging to make sure that implementations for different models, instruments, and computational architectures will be consistent. It will be difficult to train and support developers and users to develop and use implementations in such a setting.

Scriptable and configurable components and set-ups introduce varying amounts of overhead in C++ and other implementation languages. If components can be scripted and configured separately, care has to be taken so that scripting and configuration are consistent and that the developers and users do not have to learn and use different scripting and configuration languages for each component. If each component embeds a separate scripting layer or interface, it can become challenging to coordinate all the different scripting layers and interfaces. If each component has a separate Python interface, one now needs to build the entire system from Python, with separate knowledge of each Python interface, and there is a question how the different components can work on shared data or how the data is moved between the different components.

If some or all of the components are written in Python, there is the concern that pure Python implementations could be too slow or not performant enough, while using standard or specialized libraries like NumPy, JAX, TensorFlow, PyTorch, and others requires developers and users to become familiar enough with the different libraries to use them, and in particular to use them efficiently enough for purpose. Similarly, if specialized components are written in C++, C, C#, FORTRAN because of speed or interface concerns, at least developers will need to be proficient in these various programming languages and development styles, while at the same time ensuring that the components will work well together as part of the larger system. The challenges become even more substantial if different operating systems need to be supported and if performant implementations on different target computing architectures will require different libraries or set-ups (CUDA for NVIDIA GPU, OpenCL for other GPUs, OpenMP for shared-memory distributed computing, MPI for distributed computing, etc.).

These and other considerations often force the use of a small number of paths (1000-5000 in CVA applications) for MC implementations because the architecture cannot support more or the architecture can only provide these few paths in the given computational budget. However, MC estimates using such small number of paths are often unreliable and exhibit large variance, and often require specialized, one-off methodologies to address or mitigate reliability and variance concerns (for instance, using control variates that are strongly tailored to model and instrument, with tests of quality, reliance, and accuracy of varying frequency outside of production use).

In this paper, we use code generated GenSimFW parametric MC pricers together with other components for some calibrations, and we have used TensorFlow computational graphs generated by direct execution for some tests. Using GenSimFW in this way addresses the above concerns:

- The GenSimFW based implementations are component based.
- Everything is steered and configured in one place through Python and GenSimFW configuration and set-up. Users in general do not need to be proficient in the underlying libraries

or handle different aspects beyond configuration and scripts.

- Random numbers (Pseudo- or Quasi- or Pseudorandomized Quasi-Random numbers) can be generated by the component internally, by an external component, or precomputed in any fashion and provided to the component from outside.
- For global or local optimization, we can use outside optimizers implemented in or interfaced to in Python, such as the SciPy optimization suite or openly accessible ones like NAG's DFOLS, or use internally developed ones (we developed and are using ICDE as a differential evolution variant in our case).
- Using GenSimFW allows one to separate concerns, large parts of the complexity are addressed by the framework and as such do not need to be addressed by users of the framework.
- GenSimFW translates the script which is written in a common API that is supported by all its backends (and could be supported by others libraries as well) and is then translated into appropriate TensorFlow 1<sup>2</sup>, NumPy, or JAX function calls so that users do not need to know how to implement in TensorFlow, NumPy, or JAX. GenSimFW is extensible and additional functions can be provided within or outside the script and/or framework.
- The current backends TensorFlow, NumPy, and JAX run on many current computational architectures (CPU, GPU, TPU, Intel, PowerPC, etc.) and different operating systems and are highly optimized and vectorized. Most time is spent in computational kernels and data handling, not in scripting. There are optimized versions for particular settings and architectures that still provide the same general API. There are also optimizing variants such as Numba or similar. The NumPy interface is based on data structures that are common and shared between Python and C/C++ versions so that data can be efficiently communicated, transferred, and used in different languages. Many libraries provide a partial or complete NumPy implementation. Typically, the libraries rely on BLAS, XLA, and similar library interfaces, and more efficient and specialized versions can be used that implement the same interface.
- Different backends provide additional features. For instance, TensorFlow 1 provides optimizations and compilation for computational graphs<sup>3</sup>, TensorFlow 1 has algorithmic differentiation on the level of computational graphs<sup>4</sup> and JAX has JIT compilation to XLA, vectorization, and algorithmic differentiation<sup>5</sup>. In this way, we can take advantage of additional features of the backends in a generic way. Different backends also have ways to run different precisions and bitnesses, allowing lower precision results to be computed substantially faster.
- Using GenSimFW in the direct execution mode, we have overhead in the generation of the TensorFlow computational graph and in the execution of the NumPy or JAX computation (since direct execution combines both parsing and interpretation of the script with execution of the actual computation or graph generation), but not in the TensorFlow computations based on the generated computational graph.

---

<sup>2</sup>Or version 1 compatibility part of TensorFlow 2

<sup>3</sup>Native TensorFlow 2 provides optimization and compilation for Python scripts that use TensorFlow functions, through tracing.

<sup>4</sup>TensorFlow 2 implements algorithmic differentiation through tracing and tapes, which incurs additional overhead and work and makes adding higher order derivatives much less convenient compared to TensorFlow 1.

<sup>5</sup>All implemented through tracing and optimizing over a different, internal, representation JaxPR, which can not be generated easily from the outside or executed easily by itself.

- Tracing through the direct execution mode functions will result in complicated traces that do not reflect a good trace of the actual computation. GenSimFW could directly generate computational graphs, ASTs, or tapes for libraries that support algorithmic differentiation or Just-In-Time compilation (just as it generates computational graphs in and for TensorFlow1) but unfortunately XLA, JaxPR etc. cannot be easily generated and worked with from outside JAX or TensorFlow.
- However, using GenSimFW in code generation mode, using the generated modules results in no or minimal overhead, since the generated code are specialized as much as possible. The generated modules are straight-line code and are quite efficient, leading to simulation and pricing that is sufficiently fast for many purposes, with sizeable batches of paths computed at the same time, depending on model and instrument complexity ranging from 50,000 to more than a million or more paths.
- Being Python with well-known libraries, the generated code can be inspected and debugged easily on its own, with standard Python editors and debuggers.
- Computational graph generation in TensorFlow 1 is more efficient through the code generated Python-TensorFlow scripts than through the direct execution, but not dramatically so. Appropriately code generated Python JAX scripts can be traced, JITed, JAX vectorized, and JAX differentiated, trading time and memory needs for tracing, JIT, and algorithmic differentiation for much more efficient execution and the computation of appropriate derivatives, subject to limitations imposed by JAX and its implementations.

We thus obtain parametric pricers and calibration set-ups with a much lower barrier to entry and a much simplified implementations of models and instruments, allowing us to simulate and price a large variety of models, and calibrate a large variety of models sufficiently efficiently in this way (in a minute or less in many of our tests).

## 6 Learning Parametric Pricers through Parametric Differential Machine Learning for Pricing and Calibration

Often, one has some stochastic model (such as a system of SDEs, ODEs, and other Markovian updates) with one or several model parameters, and one is interested in the efficient estimation of expectations and conditional expectations (in quantitative finance, these are current prices or future (conditional) prices). For situations such as counterparty or market risk, one often needs expectations of payoffs conditional on the Markovian state at some intermediate time. Savine and Huge demonstrated the potential of a Differential Machine Learning technique, where a neural network is trained on samples of the payoff, the Markovian state to be conditioned on, and the path-wise derivatives of the payoff with respect to the Markovian state. For many stochastic processes and settings (corresponding to parabolic equations satisfying certain conditions), the dependency on state becomes smooth after infinitesimal small time. However, one is often interested in the behavior of the conditional expectation in dependence of the model parameters or parameters involved in the payoff, not only conditional on the Markovian state. Therefore, we introduced Parametric Differential Machine Learning (PDML) in [PH23] where we vary model and/or contract parameters either without varying Markovian state or together with varying Markovian state.

More formally, parametric differential machine learning (PDML) approximates the conditional expectation  $E[Y|X]$  by training a deep neural network  $N(X; \Theta)$  with parameters  $\Theta$

- Input: Script and set-up information
- Preprocessing script, classifying & splitting, parsing appropriate parts, analyze, rewrite
- Direct execution mode:
  - TensorFlow 1 and TensorFlow 2 Version 1 compatibility layer
    - \* Generate TF1 computational graphs (CGs)
    - \* User can post-process and/or augment CGs with TF (e.g. algorithmic differentiation)
    - \* User runs CGs in TF, extracts, and post-processes results
  - NumPy or JAX
    - \* Call appropriate NumPy or JAX functions to perform computations
    - \* User extracts and post-processes results
- Code generation mode:
  - TensorFlow 1 and TensorFlow 2 Version 1 compatibility layer
    - \* Generate specialized code that will generate TF1 CGs
  - NumPy or JAX
    - \* Generate specialized code that will call appropriate NumPy or JAX functions to perform computations
    - \* Generated code is straight line and easier to trace and debug (so user can use JAX features or debugger)

Figure 4: GenSimFW modes

(typically weights and biases) on  $N_S$  joint samples  $\{(X^i, Y^i, DY^i), i = 1, \dots, N_S\}$  with  $X^i = (X_j^i, j = 1, \dots, N_X)$  samples of the conditioning variables (Markovian state, model parameters, and/or contract parameters) each of size  $N_X$ ,  $Y^i = (Y_j^i, j = 1, \dots, N_Y)$  corresponding samples of the output variable(s) – typically payoffs – each of size  $N_Y$ , and  $DY^i$  denotes the collection of path-wise differentials  $\frac{\partial Y_j^i}{\partial X_I^i}$  where  $I$  and  $J$  specify which partial differentials of output variables with respect to which conditioning variables are used in the training. The loss function in PDML is

$$\Theta_N^{*,PDML} = \arg \min_{\Theta_N} E \left[ |Y - N(X; \Theta_N)|^2 + \sum_{i,j} \lambda_{ij} \left| DY_{ij} - \frac{\partial N(X; \Theta_N)_{I(i)}}{\partial X_{J(j)}} \right|^2 \right]. \quad (30)$$

We denote  $DY_{ij} = \frac{\partial Y_{I(i)}}{\partial X_{J(j)}}$  where mappings  $I$  and  $J$  specify which partial derivatives are used in the loss function.

In [PH23], we showed how PDML can be trained to learn the price of caplets as a function of contract and/or model parameters. We can use uniform sampling distributions to sample model or contract parameters for the parametric simulation to generate samples with those conditioning variables. However, if the magnitude of  $Y$  varies substantially for different parameter regions in the parameter set, training on uniformly sampled parameters might lead to worse fit in the

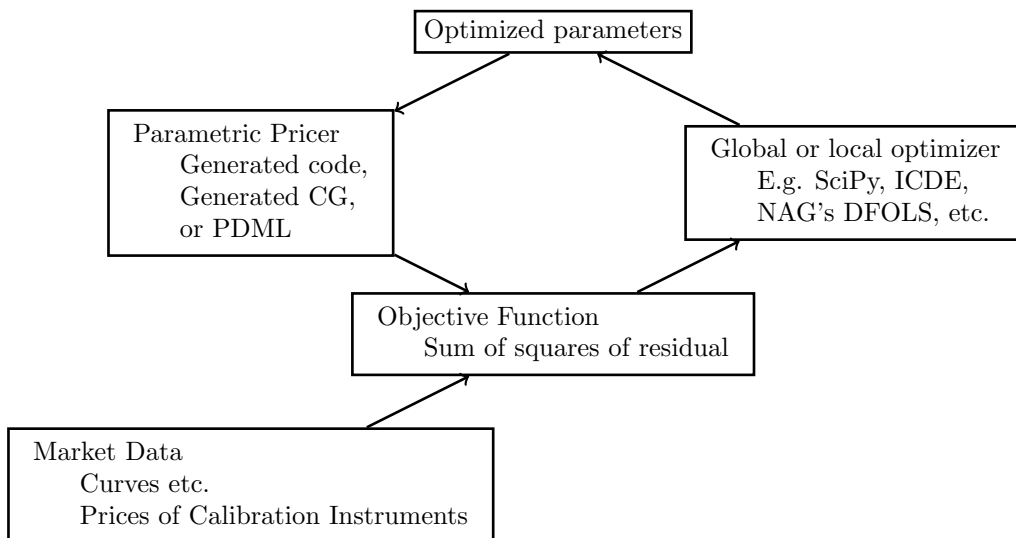


Figure 5: Calibration with Parametric Pricers

parameter regions where the magnitude of  $Y$  is smaller. In such cases, one can use adaptive sampling to improve fit in such regions, as demonstrated in [PH23]. In [PH23], we observed that using differentials in the training leads to faster convergence of price predictions and risk sensitivities predictions and to increased accuracy of prices and sensitivities.

Once trained, the deep neural networks can be used as fast parametric surrogates and pricers. The parametric pricer so obtained can be used inside a global optimizer such as ICDE to find optimized parameter sets for a variety of calibration objective functions. Such a calibration process uses random seeds at several points, when generating parameters for the sampling, simulating the stochastic processes, initializing weights and biases for the training of the DNN, and when ICDE generates new populations by random sampling and cross-over. Different seeds will in general lead to different optimized parameter sets that lead to different accuracies. Instead of trying to minimize randomness, we can use randomness and replication to obtain more robust calibration processes. We test the accuracy of the parametric pricers by some Monte-Carlo estimates on the last optimized parameters. Based on these indicators of accuracy, we studied two approaches, a ‘best seed’ approach and an ensemble approach, to obtain a more robust calibration based on several random replications of training a surrogate and calibration by optimizing over that surrogate. We used these calibration approaches to calibrate models with constant parameters against single maturity data and to calibrate models with piece-wise constant parameters against data for several maturities, with a bootstrapping approach where robustified calibration as just discussed is used to determine parameters up to the first maturity and then between maturities. We demonstrated these calibration approaches in [PH23] on the example of linear benchmark forward rate local volatility with uncorrelated CIR SV.

In this paper, we will apply these approaches to calibrate some One Factor Cheyette models with various functional forms for the local volatility combined with various stochastic volatility or variance SDEs.



## 7 Calibration using code generated MC pricers vs. calibration with PDML

PDML calibration approaches require implementations where derivatives are well-behaved, ML approaches require adaptations so that training of surrogates is fast, efficient, and converges well and where convergence and accuracy can be easily checked. In addition, these approaches sometimes only work really well if there are not too many parameters or where dimensionality reduction techniques can be applied such as differential PCA. Also, for instance, if the location of interpolation points are parameters, derivatives with respect to the interpolation point locations typically cannot be computed by the standard algorithmic differentiation of computations. Computations for different locations or numbers of interpolation points often require different implementations. There are also cases in which the results do not smoothly depend on at least some of the parameters, either locally or globally. Such situations pose particular challenges for PDML and similar approaches, complicating the sampling but also the accurate computation and use of derivatives. When PDML methods cannot be applied as easily (or the user or developer does not want to go through the trouble and effort to implement and to test such methods), calibration around code generated MC pricers can be an efficient and useful alternative. Its use provides great flexibility and convenience and allows straightforward calibrations in settings that were previously infeasible or too inefficient.

For instance, for the piece-wise linear benchmark forward rate local volatility setting where we optimize over the different pieces, PDML approaches can be challenging to apply, but calibration around code-generated MC pricers is straightforward and applicable. Thus, we applied calibration around code-generated MC pricer code for this and several of the other settings, using derivative-free ICDE variants for the work in this paper.

## 8 Numerical Results: Pricing and Calibration

In our previous paper [PH23], we demonstrated the calibration of caplets with tenor 3M for maturities ranging from 1yr to 6yr for Cheyette model with linear benchmark forward rate local volatility (LinBRLV) and (uncorrelated) CIR SV. In particular, we showed the calibration results for single-seed as well as robustified optimizations. We also considered model calibrations to single maturities as well as piece-wise calibrations to several maturities. We observed that except for 1yr maturity, the price difference between market prices from the CapFloor volatility surfaces and MC prices with calibrated parameters is well within 2 standard error bars for most of the strikes and all the strikes near ATM. For the 1yr maturity, the Cheyette model with linear benchmark forward rate local volatility could not be calibrated well across all strikes - it was not able to reprice the middle strikes (200-300bps) at the same time as repricing the other strikes and the tails, as shown in Figure 6. Here, MKT denotes the market price of the caplet for the corresponding strike and MKT - MC shows how well the optimized parameter set with enough samples of MC (approximate ground truth) approximates the MKT prices. Here, the optimized parameter set is obtained by best seed PDML calibration approach proposed in our previous paper [PH23]. In Figure 6, we can see that approximate ground truth values obtained using optimized parameter set did not reprice target prices (MKT) well in some ranges which could indicate some limitations and properties of the chosen model setting.

In this paper, we consider Cheyette model with other functional forms for the local volatility and with uncorrelated and correlated CIR SV and with correlated lognormal SV with quadratic drift (QDLNSV). We investigate whether calibration in these different model settings improves the repricing of the market volatility slice compared to the less-than-perfect repricing for 1Y

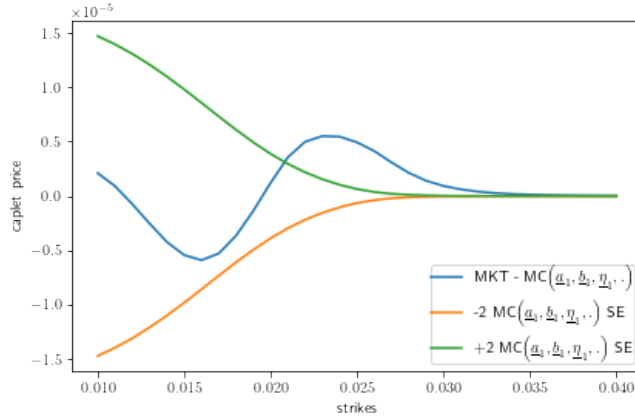


Figure 6: 1yr Maturity Calibration using Best Seed PDML Calibration Approach for Cheyette Model with Linear Benchmark Forward Rate Local Volatility (LinBRLV) and CIR SV. Figure from [PH23].

caplets on 3M rates under the model setting in [PH23]. Figure 7 summarizes the calibration quality of a set of such forms considered in this paper.

Model Setting	Fixed Parameters
LinBRLV + CIRSV	$\lambda = 0.03, \theta = 0.2$
LinBRLV	$\lambda = 0.03, \theta = 0.2$
LinBRLV + CorCIRSV	$\lambda = 0.03, \theta = 0.2$
PwLinBRLV + CIRSV	$\lambda = 0.03, \theta = 0.2, K_1 = 0.95\text{ATM}, K_2 = \text{ATM}, K_3 = 1.05\text{ATM}$
LinSRLV + CIRSV	$\lambda = 0.03, \theta = 0.2$
LinXLV + QDLNSV	$\lambda = 0.025, \kappa_1 = 0.25, \kappa_2 = 0.25$
LinBRLV + QDLNSV	$\lambda = 0.025, \kappa_1 = 0.25, \kappa_2 = 0.25$
LinSRLV + QDLNSV	$\lambda = 0.025, \kappa_1 = 0.25, \kappa_2 = 0.25$

Table 1: Fixed parameters for each model setting shown in Figure 7.

Model Setting	Parameter Bounds
LinBRLV + CIRSV	$a : [0.0001, 0.015], b : [-0.5, 0.5], \eta^6 : [0.1, 0.63]$
LinBRLV	$a : [0.0001, 0.015], b : [-0.5, 0.5]$
LinBRLV + CorCIRSV	$a : [-0.1, 0.1], b : [-0.1, 0.1], \eta^6 : [0.1, 0.63], \rho : [-0.9, 0.9]$
PwLinBRLV + CIRSV	$a_1 : [10^{-6}, 0.5], a_2 : [10^{-6}, 0.5], a_3 : [10^{-6}, 0.5], \eta^6 : [0.1, 0.63]$
LinSRLV + CIRSV	$a : [0.0001, 0.015], b : [-0.5, 0.5], \eta^6 : [0.1, 0.63]$
LinXLV + QDLNSV	$a : [-0.1, 0.1], b : [-0.1, 0.1], \beta : [-0.1, 0.1], \epsilon : [0.1, 1.0]$
LinBRLV + QDLNSV	$a : [-0.1, 0.1], b : [-0.1, 0.1], \beta : [-0.1, 0.1], \epsilon : [0.1, 1.0]$
LinSRLV + QDLNSV	$a : [-0.1, 0.1], b : [-0.1, 0.1], \beta : [-0.1, 0.1], \epsilon : [0.1, 1.0]$

Table 2: Parameter bounds used in calibration for each model setting shown in Figure 7.

<sup>6</sup> The parameter bounds for the volatility of variance are chosen such that the Feller condition is satisfied.

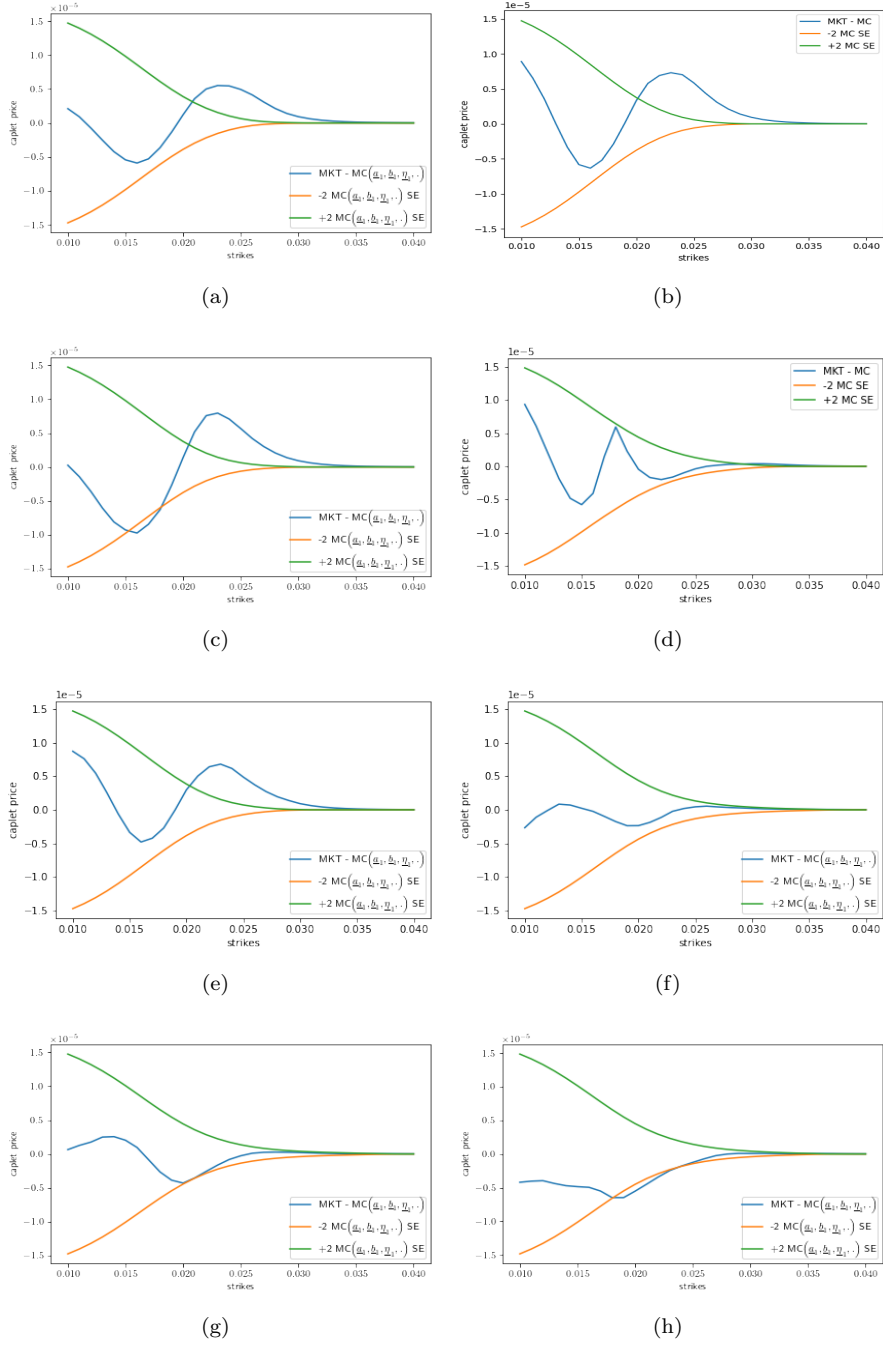


Figure 7: Calibration results for 1yr maturity caplets under various model settings. (a) LinBRLV + CIR SV (b) LinBRLV (c) LinBRLV + CorCIRSV (d) PwLinBRLV + CIR SV (e) LinSRLV + CIR SV (f) LinXLV + QDLNSV (g) LinBRLV + QDLNSV (h) LinSRLV + QDLNSV.

Model Setting	Calibrated Parameters	Good Fit?
LinBRLV + CIRSV	$a = 0.00832, b = -0.19208, \eta = 0.56724$	✗
LinBRLV	$a = 0.00762, b = -0.15945$	✗
LinBRLV + CorCIRSV	$a = 0.00679, b = -0.09999, \rho = -0.46437, \eta = 0.31777$	✗
PwLinBRLV + CIRSV	$a_1 = 0.00615, a_2 = 0.00361, a_3 = 0.00511, \eta = 0.62762$	✓
LinSRLV + CIRSV	$a = 0.00766, b = -0.15588, \eta = 0.34177$	✗
LinXLV + QDLNSV	$a = -0.00522, b = 0.08982, \beta = 0.09999, \epsilon = 0.55189$	✓
LinBRLV + QDLNSV	$a = -0.00665, b = 0.09999, \beta = 0.09999, \epsilon = 0.60884$	✓
LinSRLV + QDLNSV	$a = -0.00674, b = 0.09999, \beta = 0.09999, \epsilon = 0.62731$	✗

Table 3: Calibrated parameters for each model setting shown in Figure 7.

From the summary figure, we see that the model settings in panels (d), (f), and (g) lead to calibrations that reprice volatility slice market data within two Monte Carlo Standard Error estimates, while the other settings do not. We will now discuss particular calibrations in turn.

Firstly, as a straightforward extension of the Cheyette model setting as in [PH23], we consider a Cheyette model with piece-wise linear benchmark forward rate local volatility (PwLinBRLV) together with an uncorrelated CIR SV. We use an MC calibration approach with code generation for this model setting. We chose a set of 3 strikes to form a piece-wise linear function and these strikes were chosen based on the ATM strike, in particular, we chose  $K1 = 0.95 \times \text{ATM}$ ,  $K2 = \text{ATM}$ , and  $K3 = 1.05 \times \text{ATM}$ . In Figure 8 we show the calibration result of 1yr maturity for this new model setting. In this figure, MC denotes the MC with enough samples computed using the

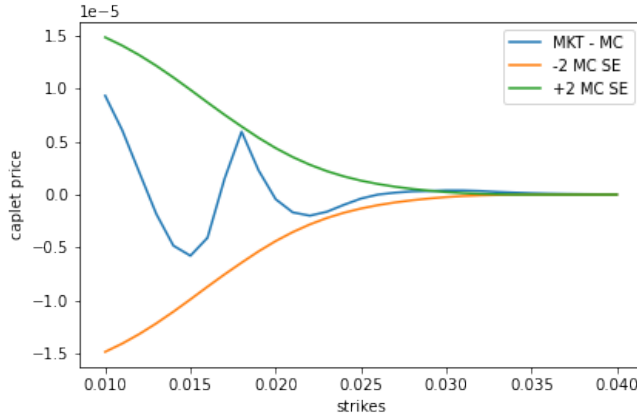


Figure 8: 1yr Maturity Calibration using MC Calibration for Cheyette Model with Piece-wise Linear Benchmark Forward Rate Local Volatility form (PwLinBRLV) and uncorrelated CIR SV.

optimized parameter set obtained by MC calibration approach. We can clearly see that the price difference between MKT and MC is well within 2 standard error bars for all the strikes. This model setting improves the repricing and calibration quality over the previous model setting. However, choosing the appropriate set of strikes to use to define the piece-wise linear function can be a challenge and one has to choose them by trial and error. It would be good to have a model setting in which one does not need to choose such details ad-hoc or such details are picked automatically while still leading to consistent results.

Next, we consider a linear short rate local volatility functional form (LinSRLV) together with uncorrelated CIR SV. The calibration result is shown in Figure 9. We can see that this linear short rate volatility functional form with uncorrelated CIR SV does not replicate the market prices in the middle of the plotted strikes well, similar to the results we obtained in [PH23].

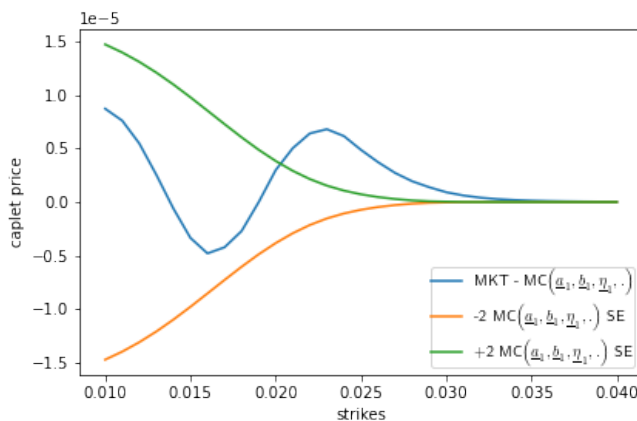


Figure 9: 1yr Maturity Calibration using Best Seed PDML Calibration Approach for Cheyette Model with Linear Short Rate Local Volatility form (LinSRLV) and uncorrelated CIR SV.

Then, we consider the linear Cheyette factor local volatility functional form (LinXLV) with a correlated lognormal SV with quadratic drift (QDLNSV). This form of lognormal SV was introduced in [SR23a]. The calibration result is shown in Figure 10. We can see that the price difference between MKT and MC is well within 2 standard error bars for all the strikes and thus fits market prices well even in the region where linear benchmark forward rate local volatility and uncorrelated CIR SV was unable to do so.

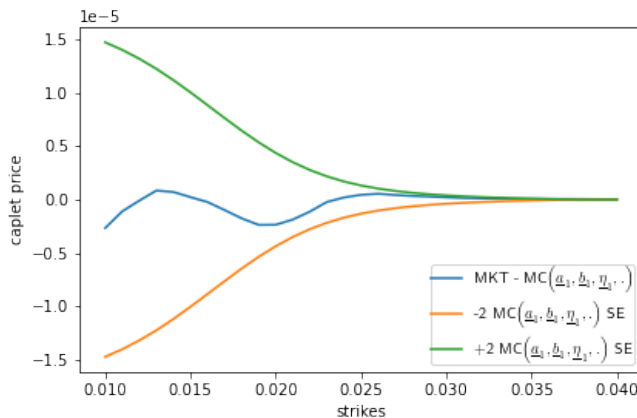


Figure 10: 1yr Maturity Calibration using Best Seed PDML Calibration Approach for Cheyette Model with Local Volatility Linear in Cheyette Factor (LinXLV) and Correlated Lognormal SV with Quadratic Drift (QDLNSV).

From our numerical investigation so far, we observe that the piece-wise linear benchmark

forward rate local volatility form (PwLinBRLV) with uncorrelated CIR SV and two forms of local volatility (linear Cheyette factor local volatility - LinXLV - or linear benchmark rate local volatility - LinBRLV) with lognormal SV with quadratic drift (QDLNV) are the only forms which priced the 1yr maturity close to the market prices across all the strikes.

Next, we investigate if we can calibrate well using benchmark forward rate and short rate volatility functional forms when used with the lognormal SV with quadratic drift (QDLNSV). Figures 11 and 12 show the calibration results for benchmark rate volatility functional form with QDLNSV and short rate volatility functional form with QDLNSV, respectively. We can see that in Figure 11 benchmark rate volatility functional form with QDLNSV repriced market volatility surface prices well within 2 standard error bars, thereby improving accuracy over benchmark rate vol model with uncorrelated CIR SV. In Figure 12, we can see that the short rate volatility form with QDLNSV priced close to 2 standard error bars in the middle of the strikes and better fit when compared to short rate vol with uncorrelated CIR SV in Figure 9. So, this shows for 1yr maturity for caplets, lognormal SV with quadratic drift can fit the vol smile well and better than CIR SV can.

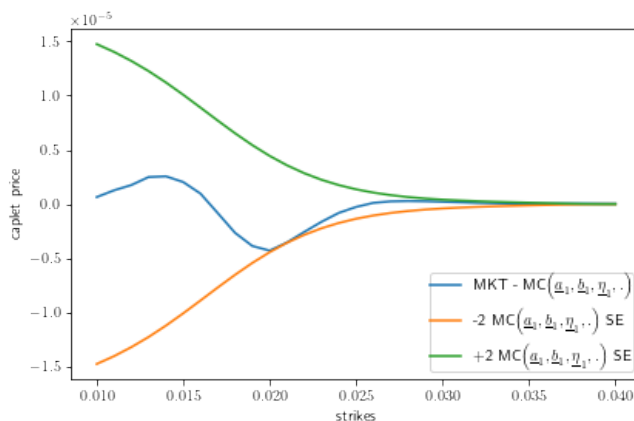


Figure 11: 1yr Maturity Calibration using Best Seed PDML Calibration Approach for Cheyette Model with Linear Benchmark Rate Volatility form (LinBRLV) and Lognormal SV with Quadratic Drift (QDLNSV).

Finally, in our previous paper [PH23] we observed that the linear benchmark rate volatility functional form (LinBRLV) with uncorrelated CIR SV calibrates well and close to 2 standard error bars for maturities ranging from 2yr to 6yr. Here, we investigate whether we can calibrate well for later maturities (2yr to 6yr) with linear benchmark rate volatility form (LinBRLV) with QDLNSV, in addition to the 1yr calibration we already covered. We follow the calibration approach outlined in [PH23] for calibrating multi-maturity data and settings. Figure 13 compares the price graphs of caplets of maturities ranging from 1yr to 6yr from MC with enough samples (treated as approximate ground truth) and market prices. Figure 14 shows the price differences between MC (approximate model ground truth) and market prices for various maturities. Both of these figures show linear benchmark rate volatility functional form together with correlated QDLNSV calibrated well within or close to 2 standard error bars for all the strikes and for all the maturities considered.

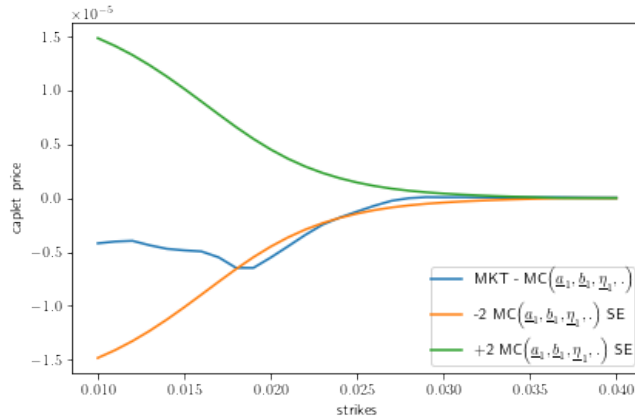


Figure 12: 1yr Maturity Calibration using Best Seed PDML Calibration Approach for Cheyette Model with linear Short Rate Volatility form (LinSRLV) and Lognormal SV with Quadratic Drift (QDLNSV).

## 9 Conclusions

In this paper we studied whether one-factor Cheyette models with different forms of local volatilities and/or stochastic volatilities can calibrate to short maturity caplet smiles across a wide range of strikes, unlike the one-factor Cheyette model with linear benchmark rate local volatility and uncorrelated CIR stochastic variance studied in [PH23]. We tested several local volatility forms and stochastic volatility and variance forms. We could do so conveniently and efficiently through the generic simulation scripting framework and two calibration approaches - one calibrating around parametric simulation prices from code generation or computational graph generation as introduced in this paper, while the other uses parametric differential machine learning (PDML) as introduced in [PH23]. The scripting framework allows the easy and convenient specification of the models and instruments and the code generation and calibration set-ups lead to calibrations that work well with relatively small computational effort and often return calibrated parameters within a minute.

We identified several model settings that calibrate well to the short maturity data, in particular a model setting with a local volatility that is piece-wise linear in the benchmark forward rate together with an uncorrelated CIR stochastic variance and several model settings with a correlated lognormal stochastic volatility with quadratic drift (as introduced in [SR23a]) combined with various local volatility forms, including the one that is linear in the benchmark forward rate. We prefer the lognormal stochastic volatility with quadratic drift since then we do not need to find the appropriate anchor strikes for the piece-wise linear local volatility by trial and error, instead of mostly automatically through some optimization. Benchmark forward rate formulations are preferred since they can be more easily fitted.

Similar case and modeling studies can be performed with other model types and instruments.

We see that the presented generic simulation, pricing, and calibration frameworks make such calibration and modelling studies feasible, efficient, and even easy. Based on their results, one can develop and fine tune appropriate production models for a variety of markets and instrument features.

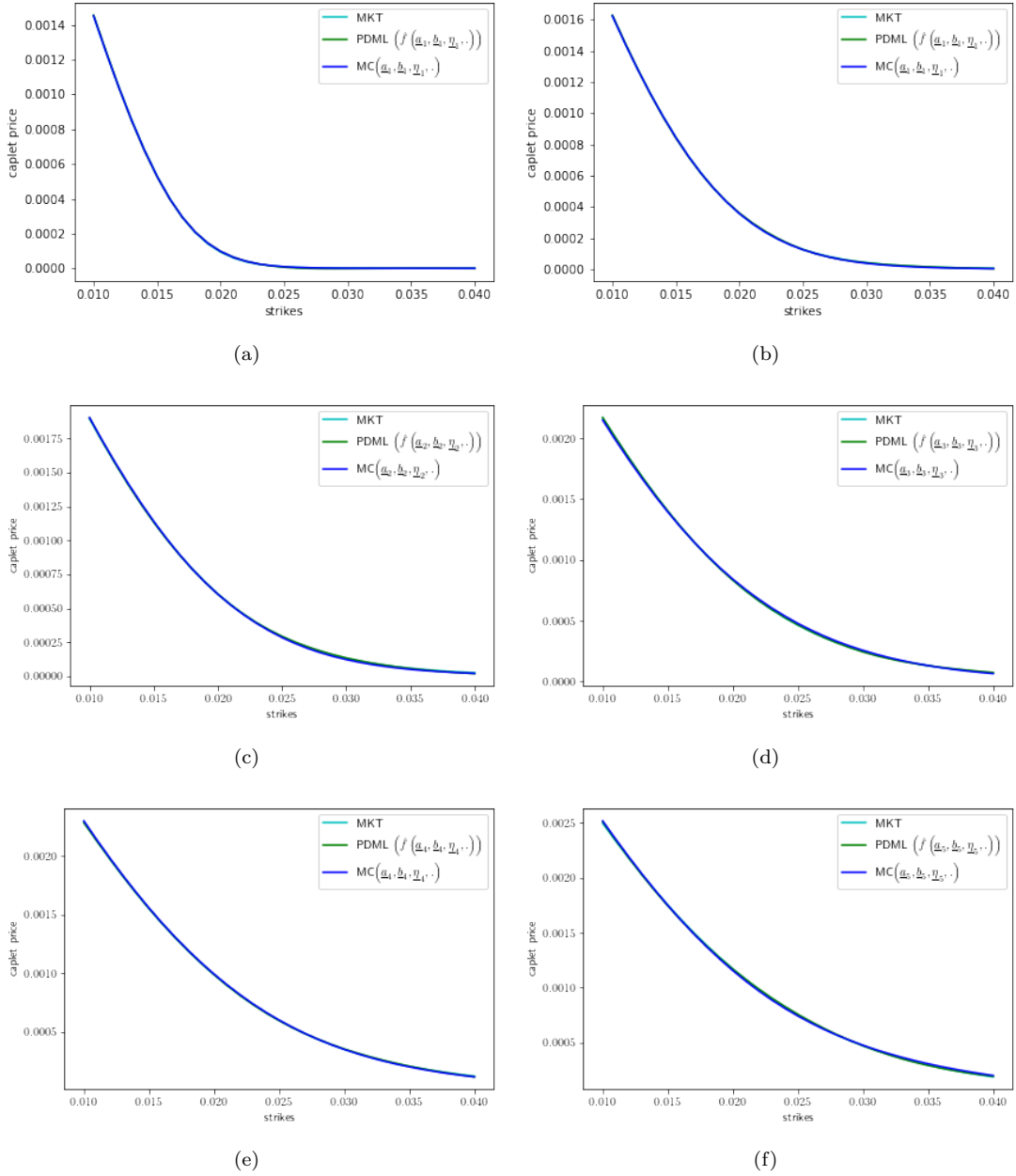


Figure 13: Calibration with Best Seed PDML Calibration Approach for Cheyette Model with Linear Benchmark Rate Volatility (LinBRLV) and Correlated Lognormal SV with Quadratic Drift (QDLNSV). Plots show Prices from MC (approximate ground truth) at Optimized Parameters Compared to Market Prices for various Maturities. (a) 1yr Maturity (b) 2yr Maturity (c) 3yr Maturity (d) 4yr Maturity (e) 5yr Maturity (f) 6yr Maturity.



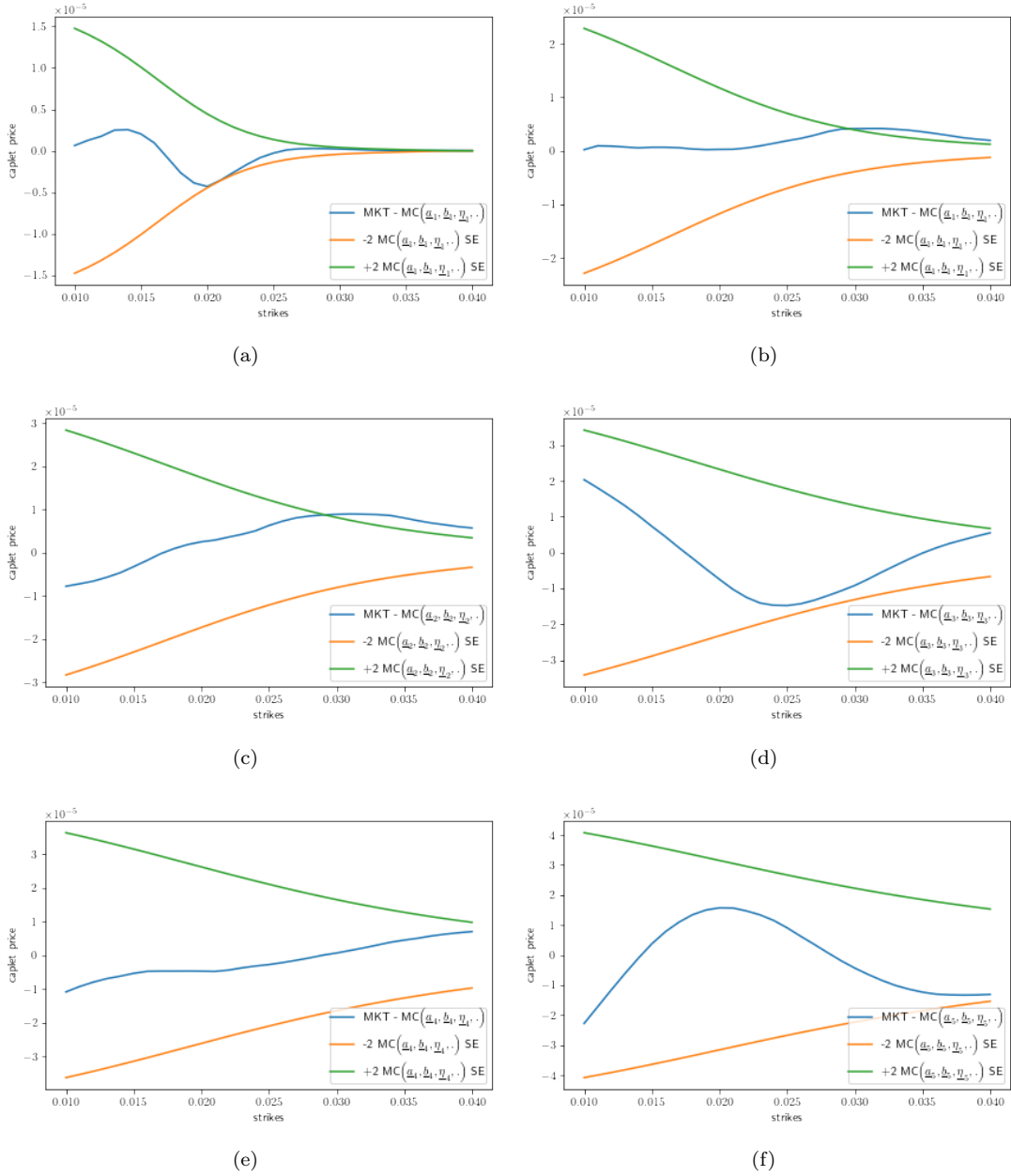


Figure 14: Calibration with Best Seed PDML Calibration Approach for Cheyette Model with Linear Benchmark Rate Volatility form (LinBRLV) and Correlated Lognormal SV with Quadratic Drift (QDLNSV). Plots show Price differences between MC (approximate ground truth) at Optimized Parameters and Market Prices for various Maturities. (a) 1yr Maturity (b) 2yr Maturity (c) 3yr Maturity (d) 4yr Maturity (e) 5yr Maturity (f) 6yr Maturity.

### Acknowledgments:

The authors thank Vijayan Nair for his comments and suggestions regarding this research. Any opinions, findings and conclusions or recommendations expressed in this material are those of the authors and do not necessarily reflect the views of Wells Fargo Bank, N.A., its parent company, affiliates and subsidiaries.

## References

- [AP10] L Andersen and V Piterbarg. *Interest Rate Modeling*. Atlantic Financial Press: London, 2010.
- [Chi12] Messaoud Chibane. Explicit volatility specification for the linear cheyette model. *Available at SSRN 1995214*, 2012.
- [DRP13] Nick Deguillaume, Riccardo Rebonato, and Andrey Pogudin. The nature of the dependence of the magnitude of rate moves on the rates levels: a universal relationship. *Quantitative Finance*, 13(3):351–367, 2013.
- [Hen10] Marc P.A. Henrard. The irony in the derivatives discounting, Part II: The crisis. *Wilmott Journal*, 2:301–316, 2010. Also available at SSRN.
- [Hoo11] Bart Hoorens. *On the Cheyette short rate model with stochastic volatility*. PhD thesis, Delft University of Technology, 2011.
- [PH23] Arun Kumar Polala and Bernhard Hientzsch. Parametric differential machine learning for pricing and calibration. *arXiv preprint arXiv:2302.06682v2*, 2023.
- [SR23a] Artur Sepp and Parviz Rakhmonov. A Robust Stochastic Volatility Model for Interest Rate Dynamics. *Risk Magazine*, 2023.
- [SR23b] Artur Sepp and Parviz Rakhmonov. What Is a Robust Stochastic Volatility Model. *SSRN*, 2023.